Growth and characterization by STM of BiCo222 crystal objects: whiskers and bows

M. BURDUSEL[a], L. MIU[a], P.H. ZHAO[b], W. YAN[b], Y.L. HAN[b], J.C. NIE[b], P. BADICA[a*]
[a]*National Institute of Materials Physics, Atomistilor 105bis, Magurele 077125, Romania*
[b]*Beijing Normal University, Physics Department, Beijing 100875, Peoples R China*

Lamellar crystal objects such as straight, curved or kinked whiskers, bows and objects with missing stripes were grown in a static air atmosphere from melt-quenched substrates with starting composition $Bi_{1.5}Sr_1Ca_1Co_{0.6}O_y$. The average EDS composition of the objects is $Bi_2Sr_{0.75}Ca_{1.8}Co_{1.94}O_y$ and the crystal structure is of the phase usually denoted in the literature as $Bi_2(Sr,Ca)_2Co_2O_y$ (BiCo222). Objects of other phases were not found. Curvature is in the (*ab*)-plane. By scanning tunneling spectroscopy (STS) a semiconducting energy gap was determined at 2.41 eV.

(Received January 7, 2015; accepted March 19, 2015)

Keywords: Bi-Sr-Ca-Co-O, Whiskers, Bows, Scanning tunneling microscopy

1. Introduction

For direct energy conversion without driving parts, in the last years, layered Co-based thermoelectric oxides such as $NaCoO_x$ [1], $LaCoO_3$ [2], $Ca_2Co_3O_6$ [3], $Ca_3Co_4O_9$ [4] or the BiCo-based phases from the Bi-Sr-Ca-Co-O system [5, 6] were demonstrated to be very promising materials.

The following BiCo-based thermoelectric phases were identified [6]: $Bi_2(Sr,Ca)_2CoO_y$ (BiCo221), $Bi_2(Sr,Ca)_2Co_2O_y$ (BiCo222), $Bi_2(Sr,Ca)_2Co_5O_6$ (BiCo225). Detailed compositional and structural investigations [7-9] show that the stoichiometry of these phases might deviate from the indicated ones. For simplicity, we shall use in this work the proposed notations. According to literature [8], single crystals of BiCo-phases have a power factor S/ρ (with S being Seebeck coefficient and ρ being electrical resistivity) 5-7 times higher at 700°C than for the bulks. It results that single crystal objects are of much interest, but only few articles present their growth and characterization. Conventional plate-like rectangular BiCo-222 crystals were grown by flux [7, 9] methods adding Bi_2O_3, K_2CO_3 and KCl to reacted mixed powders of $CaCO_3$ and Co_2O_3. Ref. [6] presents growth of straight single crystal whiskers of BiCo221, BiCo-222 and BiCo-225 from melt-quenched substrates with starting cationic composition Bi:Sr:Ca:Co=1:1:1:z, z=0.5-2. Straight whiskers of BiCo-222 with Pb ($(Bi, Pb)_{2.2}(Sr,Ca)_{2.8}Co_2O_y$) were grown by the same route [8]. Whiskers were grown in a stream of oxygen [6, 8].

In this work we adopted the growth of whiskers from the melt-quenched substrates in a static air atmosphere using the 'two-crucible' arrangement described in [10]. A new starting cationic composition (Bi:Sr:Ca:Co=1.5:1:1:0.6) for the substrate is proposed. This composition results in the growth of the crystal objects of the BiCo-222 phase. Remarkable is that shapes are of straight or of highly curved/kinked whiskers or bows with the curved line in the (*ab*)-plane. We also observed bows and straight or curved whiskers with missing stripes. Morphology variations of the Bi-Sr-Ca-Co-O crystal objects are reported for the first time. They are similar as for high-T_c superconducting $YBa_2Cu_3O_y$ and $Bi_2Sr_2CaCu_2O_y$ highly curved objects [11, 12]. Curved objects can be convenient as interconnects or can help the design and integration of the electronic devices. In some situations to avoid damage during shaping of the conventional crystals, directly grown curved objects might be a useful alternative [11]. Scanning tunneling spectroscopy measurements on our objects are also presented.

2. Experimental details

Commercial powders of Bi_2O_3, SrO, $CaCO_3$ and Co_2O_3 were mixed with the starting cationic composition Bi:Sr:Ca:Co=1.5:1:1:0.6. Mixture was placed in alumina crucible and heated in the air at 1310 °C for 35 min. The heating rate from 950 to 1310 °C was 5 °/min. Melt was quenched between two massive plates of steel. Pieces of the as-prepared substrate were placed on an Al_2O_3 plate located on the bottom of a crucible inside another crucible. This 'two-crucible' arrangement is used to control spatial thermal gradients necessary for the whiskers growth. Substrates are positioned on the bottom of the inner crucible as follows: 1 substrate in the center and 4 close to the vertical walls of the inner crucible. Details of the 'two-crucible' method are presented elsewhere [10]. Samples and thermal regimes for the crystals growth are shown in Table 1 and Fig. 1.

Table 1. Samples, growth conditions, whisker length and output.

Sample	Growth conditions T_1-T_2: v	Length (mm)	Output
A	905 °C-885 °C: 0.01 °/min	-	no whiskers
B	890 °C-870 °C: 0.01 °/min	small <0.6	many small whiskers on all substrates
C	875 °C-860 °C: 0.0037 °/min	big <1.2	few big whiskers were found on the substrate located at the center of the inner crucible; a higher output is for the substrate located in the center of the crucible, but this output is less than for B

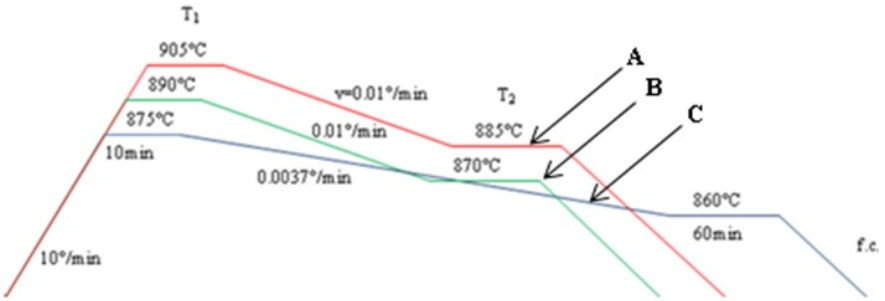

Fig. 1. Thermal regimes (A, B and C) for the growth in the static air atmosphere of BiCo222 objects from Bi:Sr:Ca:Co=1.5:1:1:0.6 substrate (see Table 1).

X-ray diffraction measurements were performed by using a Bruker-AXS D8 ADVANCE diffractometer (Cu_{Ka1} radiation, λ= 1.5406 Å). For this measurement, about 30 straight and curved objects were fixed with their largest surface (*ab*-plane) parallel to the surface of the glass holder.

For morphology and local compositional analysis of the substrates and of the crystal objects, a scanning electron microscope Zeiss EVO50 equipped with EDAX energy dispersive spectroscopy (EDS) system was used.

The scanning tunneling microscope (STM) was an ultra-high vacuum four-probe system from Unisoku (Japan) working at temperatures above 77 K. STM topography images were taken in the constant-current mode. Scanning tunneling spectroscopy (STS) spectra, i.e. the dI/dV-V curves at different temperatures were measured using a standard lock-in technique for 957 Hz ac modulation of the bias voltage. Objects for the STM/STS measurements were selected to have planar, clean and low roughness surfaces (usually less than 0.5 nm) using an atomic force microscope (AFM) produced by Bruker. The STM tips were obtained by chemical etching of a Pt(80%)Ir(20%)-alloy wire. STM calibration was done on graphene used also as a sample holder.

3. Results and discussion

3.1 As-prepared substrate

X-ray diffraction pattern of the melt quenched substrate is shown in Fig. 2A. Substrate is crystallized and this is confirmed by SEM (Fig. 3a). The average EDS composition of the melt-quenched substrate is $Bi_{1.5}Sr_{0.9}Ca_{1.1}Co_{0.61}Al_{0.62}O_x$ (normalized to $Bi_{1.5}$). Apart from Al, the starting cationic composition (Bi:Sr:Ca:Co=1.5:1:1:0.6) of the mixed powders is reasonably reflected in the melt-quenched substrate. Aluminum is supplied to the substrate from the alumina crucible walls during melting for the substrate preparation. We could not identify by XRD the phases from the substrate. Local EDS analysis suggests that in the substrate there are regions with different amounts of Al, while variation of Bi, Ca and Co is not high. Somehow a larger scattering in compositions is shown by Sr. Variation in local composition may point on the existence of several phases in the as-prepared melt-quenched substrate. Because the size of the grains is smaller or comparable to the size of the EDS-spot and the grain boundaries are observed with difficulty, a conclusion cannot be expressed. In ref. [6] are presented XRD patterns for melt-quenched substrates with cationic composition Bi:Sr:Ca:Co=1:1:1:z, z=0.5-2. Only for high Co amounts ($z \geq 1.75$) substrate is crystallized. Phases were not identified. For small z-values substrate is amorphous. Therefore, situation is different than in our case, i.e. for a small amount of Co our substrate is crystallized, despite the fact that in a rough approximation, preparation of the melt-quenched substrates was not so different. Namely, in both cases it was performed in the air at 1310 °C for 35 min. in ref. [6] and at 1300 °C for 30 min. in this work. This indicates that starting composition (e.g. a higher amount of Bi as in our case) is important. We should however emphasize that other processing parameters, such as the heating rate to the melting temperature (not available for the experiments from ref. [6]), also play a

significant role in Al intake. These details will determine the status, - i.e. amorphous or crystallized, composition and location in the phase diagram - of the melt-quenched substrate. Our XRD data (Fig. 2A) clearly indicate that in our crystallized substrate Bi:Sr:Ca:Co=1.5:1:1:0.6 there are phases not present in the crystallized substrate Bi:Sr:Ca:Co=1:1:1:2 from ref. [6].

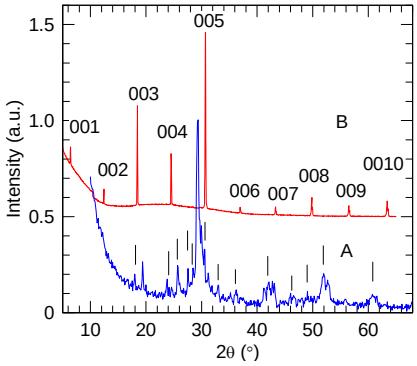

Fig. 2 XRD patterns of: (A)- as-prepared our melt-quenched substrate (positions of the peaks observed in the XRD of the crystallized Bi:Sr:Ca:Co=1:1:1:2 melt-quenched substrate from ref. [6] are indicated with vertical lines); (B)- BiCo222 objects grown in this work.

3.2 Crystal objects

The differences encountered for our as-prepared substrate vs. those presented in literature are not essential and our substrate allows growth of crystal objects (Fig. 2B). However, there is a certain temperature window for the growth (Fig. 1, Table 1). Whiskers are not growing for the heat treatment A. A similar thermal regime B, but shifted with 15 °C to lower temperatures is providing conditions for whiskers growth. The output is relatively high, but the longest straight whiskers are of about 0.6 mm (thickness is up to 0.1 mm). If thermal regime is modified as for sample C, i.e. the total growth time is enhanced (cooling rate for sample C is 2.7 times slower than for samples A and B), longer whiskers of about 1.3 mm (thickness up to 0.1 mm) are obtained. Sample C has shown a lower output than for sample B. This is related to a lower maximum temperature in the case of sample C (875 °C) than for sample B (890 °C). A lower maximum temperature means formation of less melt droplets necessary for the growth initiation and formation of the local solid-liquid 'microcrucibles' [6] that are supporting the whiskers growth in a grass-like bottom-end fashion.

XRD patterns of our crystal objects ($Bi_{1.56}(Sr, Ca)_2Co_{1.52}O_x$, normalized to $(Sr, Ca)_2$, see below EDS data) are very similar to the XRD pattern for the BiCo222 whiskers from ref. [6]. XRD peaks (Fig. 2B) were indexed as (00l) following refs. [6, 7]. The lattice parameter *c* is 14.55 Å, and it is slightly smaller than for reported BiCo222 whiskers ($Bi_{1.93}(Sr, Ca)_2Co_{1.29}O_x$ with *c* = 14.8 Å [6]) or single crystals ($Bi_{1.64}Ca_2Co_{1.69}O_x$ with *c* = 14.661 Å [7] and $Bi_{1.68}Ca_2Co_{1.69}O_x$ with *c* = 14.668 Å [9]). If comparing results from ref. [6] and [7, 9], introduction of Sr with a larger ionic radius than Ca enhances *c*-axis. However, in our case whiskers containing Sr show a smaller *c*-axis than for the single crystals containing only Ca. This is due to a different content of Bi, Co and the presence of some Al (with ionic radius smaller than for Sr and Ca) in our whiskers. XRD indicates that preferential growth direction is in-plane, i.e. along *a* or *b* directions. The layered structure in the *c*-axis direction and along the thickness of the crystal objects is revealed also by SEM: in Fig. 3e the large whisker near the substrate shows some exfoliation.

In ref. [6] at low Co content (z = 0.5-0.75) in the substrate, BiCo221 whiskers were found. For a higher Co content, BiCo222 whiskers grow usually together with BiCo221 or BiCo225, and an annealing temperature above 900 °C is necessary to grow BiCo222 whiskers. This temperature is higher than the necessary one for the growth of any whiskers from the substrates with a low level of Co [6]. It is remarkable, that for our substrate with a relatively low Co content we obtained only objects of the BiCo222 phase. Moreover, in our case, growth window of BiCo222 objects, as already addressed, was found to be below 890 °C instead of being above 900 °C as in ref. [6]. This can be understood in the view of a higher Bi-amount in our substrate lowering the melting point and providing convenient growth conditions of the BiCo222 crystal objects at lower temperatures. However, a growth window at lower temperatures is likely suppressing the maximum growth rate of the straight whiskers from 0.08 mm/h in ref [6] (whiskers of 8 mm in length were found after 600 h annealing) to about 0.02 mm/h in our work. It is worthy to note that a significant contribution to presented behavior can be due to a different growth atmosphere: we used air, while in ref. [6] growth was performed in oxygen.

Straight and curved/kinked whiskers (Fig. 3b), bows (Fig. 3c) or whiskers with missing stripes (Fig. 3b) grow from the same substrate. Curvature if occurs, it is always in the *ab*-plane. An average EDS composition measured on different objects and at different positions on each of them is $Bi_2Sr_{0.75}Ca_{1.8}Co_{1.95}(Al_u)O_y$ (normalized to Bi_2). Cationic compositional dispersion (except for Al) is relatively low and this feature was also noted for single crystals $Bi_2Ca_{2.42}Co_{1.783}Al_{0.26}O_y$ (normalized to Bi_2) grown in ref. [7]. Single crystals from ref. [7] are considered to be Al-substituted crystals, and an enhancement of the thermopower from Al-free to Al-substituted crystals is discussed. For our objects the level of Al content detected by EDS was lower, *u*=0.06-0.12. We also observed that when the surface of the crystal object was clean, Al content was mostly in the lower limit. If the surface was apparently covered by a top layer, for few measured objects *u* was higher than 0.12. EDS Al-rich compositions were found for layered large grains from the substrate and at the root of the objects (e.g. in Fig. 3d, grain indicated with 1 has composition $Bi_2Sr_{0.94}Ca_{1.71}Co_{2.06}Al_{0.225}O_y$, normalized to Bi_2). On the other hand, droplets from the surface of the curved whisker with the missing stripe (Fig. 3b, and 3b inset) are Al and Co poor ($Bi_2Sr_{0.76}Ca_{1.2}Co_{0.3}Al_{0.07}O_y$). We note that *u*-values for the droplets are similar as for the clean whiskers. Droplets with a similar composition (Ca and Sr show a larger

fluctuation compared to the other elements) can be also observed on the substrate (Fig. 3d, indicated with 2). Considering morphology, droplets likely crystallize in the hexagonal system (Fig. 3b inset and see droplets indicated with arrows in Fig 3e). At the bases of the BiCo221 whiskers grown from the substrates with low Co amount as in our case, in ref. [6] EDS compositions measured on different grains were: $Bi_2(Sr,Ca)_{2.44}Co_{0.74}Al_{0.37}O_y$ and $Bi_2(Sr,Ca)_{3.2}Co_{0.4}Al_{2.4}O_y$, normalized to Bi_2. There are differences suggesting once more that in our case we are located in a different region of the phase diagram than in the case of ref. [6].

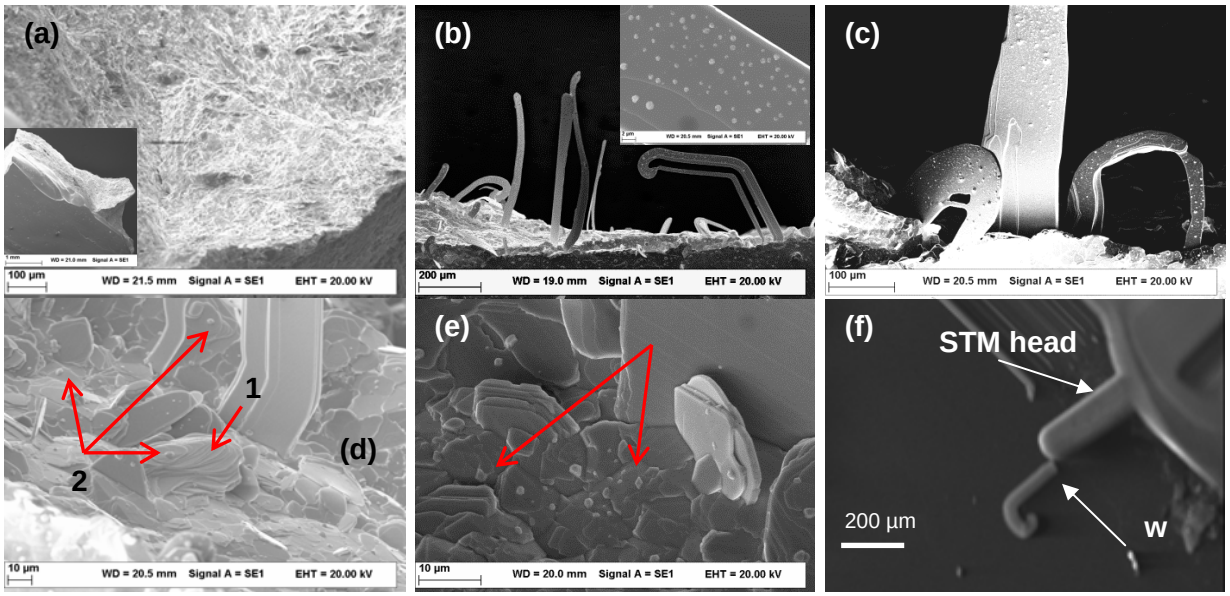

Fig. 3 SEM images of (a)- cross section of the melt-quenched substrate used in this work (inset show a general view); (b, c)- substrate and straight or curved crystal objects (inset to (b) shows in detail the surface of the curved whisker with the missing stripe); (d, e)- substrate around the base of whiskers (grains 1 and droplets 2 on the substrate are indicated with arrows, see text); (f)- curved whisker (W) BiCo222 measured by STM/STS.

Similarities in structure, morphology and growth mechanism (i.e. a solid-liquid-solid 'grass-like' mechanism) between BiCo222 curved objects from this work and high-T_c superconducting (HTS) $Bi_2Sr_2CaCu_2O_y$ or $YBa_2Cu_3O_z$ curved objects [11, 12] hints on a similar mechanism of 'curved' line formation so that the curved objects can be considered 3D epitaxial crystals 'cut' in the ab-plane from a conventional plate-like rectangular crystal or from a ribbon-like straight whisker. To obtain this effect it was argued for HTS in [11, 12] that growth rates on *a* and *b* directions can vary and, thus, can generate the curved-shape appearance. This happens due to changes of the conditions around the root of the object influencing during growth directly or indirectly the growth interface geometry and location [11]: neighboring 'microcrucibles' are changing their size, location, are merging or splitting. Further evidences are necessary to confirm also for the BiCo-based curved objects from this work the anticipated 3D epitaxial crystals nature and the mechanism of curved growth.

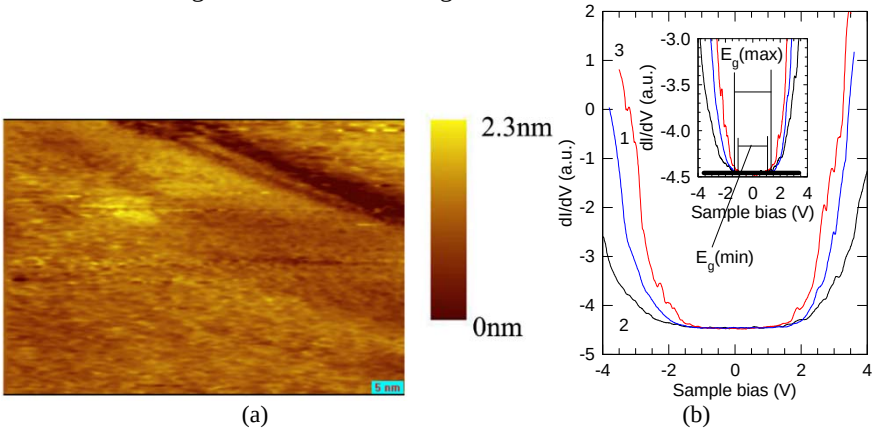

Fig. 4. (a)- STM topography image on the (ab)-plane of the curved BiCo222 whisker from Fig. 3f (color scale is for z-axis); (b) STS spectra (dI/dV – V) at different temperatures: 1 = 80 K, 2 = 125 K and 3 = 141 K. The inset shows the same spectra at a higher magnification.

A highly curved whisker measured by STM/STS is shown in Fig. 3f. The STM topography image (Fig. 4a) indicates a relatively smooth and clean surface (*ab*-plane) of the whisker. STS measurements have shown a relatively good stability and reproducibility. Examples of dI/dV - dV curves at different temperatures averaged over 5-6 measurements for different locations on the whisker are presented in Fig. 4b. The material is semiconducting with an energy gap estimated at E_g = 2.41 eV. This value is calculated as the average between the minimum (2.14 eV) and the maximum (2.68 eV) energy gap determined over all investigated temperatures (Fig. 4 inset). Energy gap was taken between points where the dI/dV - V curve deviates from a horizontal line. Variation with temperature of the STS spectra in the region outside the energy gap ascribed to DOS influence is likely significant. This may suggest that electronic structure of BiCo222 is quite sensitive with temperature. This statement requires further confirmation.

4. Conclusion

Crystal BiCo222 objects such as straight or curved/kinked whiskers, bows and objects with missing stripes were grown in static air atmosphere from a melt-quenched substrate with starting composition $Bi_{1.5}Sr_1Ca_1Co_{0.6}O_y$. Curved-line is in the *ab*-plane. Whiskers are of the BiCo222 phase. From STM/STS measurements, energy gap of BiCo222 was estimated at 2.41 eV.

Acknowledgements

Authors acknowledge Chinese–Romanian Intergovernmental S&T Cooperation Programme (Projects No. 507/22.03.2011, Romania and CH-40-12/2010, China). Work performed by the Chinese team was also supported by the National Natural Science Foundation of China (Grant Nos. 51172029, 91121012, and 10974019) and the Fundamental Research Funds for the Central Universities. Work performed at NIMP was partially supported from the project PCCE 3/2012, Romania.

References

[1] I. Terasaki, Y. Sasago, K. Uchinokura, Phys .Rev. B **56,** R12685 (1997).
[2] T. He, J.Z. Chen, T.G. Calvarese, M.A. Subramanian, Solid State Sci. **8,** 469 (2006).
[3] M. Mikami, R. Funahashi, M. Yoshimura, Y. Mori, T Sasaki, J. Appl. Phys. **94,** 6579 (2003).
[4] S. Li, R. Funahashi, I. Matsubara, K. Ueno, H. Yamada, J. Mater Chem. **9**, 1659 (1999).
[5] R. Funahashi, I. Matsubara, S. Sodeoka, Appl. Phys. Lett. **76**, 2385 (2000).
[6] R. Funahashi, I. Matsubara, M. Shikano, Chem Mater. **13**, 4473 (2001).
[7] E. Guimeau, M. Pollet, D. Grebille, M. Hervieu, H. Muguerra, R. Cloots, M. MIkami, R. Funahashi, Inorg. Chem. **46,** 2124 (2007).
[8] R. Funahashi, I. Matsubara, Appl. Phys. Lett. **79,** 362 (2001).
[9] H. Muguerra, D. Grebille, E. Guilmeau, R. Cloots, Inorg. Chem. **47,** 2464 (2008).
[10] P. Badica, K. Togano, H. Kumakura, Supercond. Sci. Technol. **17**, 891 (2004).
[11] P. Badica, A. Agostino, M.M. Rahman Khan, S. Cagliero, C. Plapcianu, L. Pastero, M. Truccato, Y. Hayasaka, G. Jakob, Supercond. Sci. Technol. **25**, 105003 (2012).
[12] S. Cagliero, E. Borfecchia, L. Mino, L. Calore, F. Bertolotti, G. Martinez-Crido, L. Operti, A. Agostino, M. Truccato, P. Badica, C. Lamberti, Supercond. Sci. Technol. **25**, 125002 (2012).

*Corresponding author: badica2003@yahoo.com